

Preprint of:

Timo A. Nieminen and Dmitri K. Gramotnev

“Non-steady-state extremely asymmetrical scattering of waves in periodic gratings”

Optics Express **10**, 268–273 (2002)

This paper is freely available at: <http://www.opticsexpress.org/abstract.cfm?URI=OPEX-10-6-268>

which includes multimedia files not included with this preprint version.

Non-steady-state extremely asymmetrical scattering of waves in periodic gratings

Timo A. Nieminen

*Centre for Biophotonics and Laser Science, Department of Physics,
The University of Queensland, Brisbane QLD 4072, Australia*

Dmitri K. Gramotnev

*Centre for Medical, Health and Environmental Physics, School of
Physical and Chemical Sciences, Queensland University of
Technology, GPO Box 2434, Brisbane QLD 4001, Australia*

Abstract: Extremely asymmetrical scattering (EAS) is a highly resonant type of Bragg scattering with a strong resonant increase of the scattered wave amplitude inside and outside the grating. EAS is realized when the scattered wave propagates parallel to the grating boundaries. We present a rigorous algorithm for the analysis of non-steady-state EAS, and investigate the relaxation of the incident and scattered wave amplitudes to their steady-state values. Non-steady-state EAS of bulk TE electromagnetic waves is analyzed in narrow and wide, slanted, holographic gratings. Typical relaxation times are determined and compared with previous rough estimations. Physical explanation of the predicted effects is presented.

OCIS codes: (050.0050) Diffraction and gratings; (050.2770) Gratings; (050.7330) Volume holographic gratings; (320.5550) Pulses

1 Introduction

Extremely asymmetrical scattering (EAS) is a radically new type of Bragg scattering in slanted, periodic, strip-like wide gratings, when the first diffracted order satisfying the Bragg condition (scattered wave) propagates parallel to the front grating boundary [1–9]. The main characteristic feature of EAS is the strong resonant increase of the scattered wave amplitude, compared to the amplitude of the incident wave at the front boundary [1–9]. Other unique features of EAS include additional resonances in non-uniform gratings [5], detuned gratings [8], in wide gratings when the scattered wave propagates at a grazing angle with respect to the boundaries [6], and the unusually strong sensitivity of EAS to small variations of mean structural parameters at the grating boundaries [9]. The additional resonances may result in amplitudes of the scattered and incident waves in the grating that can be dozens or even hundreds of times larger than that of the incident wave at the front boundary [5–9].

One of the main physical reasons for all these unusual features of EAS is the diffractive divergence of the scattered wave inside and outside the grating [2–6, 9]. Indeed,

the scattered wave results from scattering of the incident wave inside the grating, and propagates parallel to the grating. Thus, it is equivalent to a beam located within the grating, of an aperture equal to the grating width. Such a beam will diverge outside the grating due to diffraction. Therefore, steady-state EAS is formed by the two physical effects – scattering and diffractive divergence. Based on the equilibrium between these processes, an approximate analytical method of analysis of EAS, applicable to all types of waves, has been developed [2–4, 6, 8, 9].

A reasonable question is which of the EAS resonances are practically achievable? Any resonance is characterized by a time of relaxation, and if this time is too large, the corresponding resonance cannot be achieved in practice. In the case of EAS, large relaxation times may result in excessively large apertures of the incident beam being required for the steady-state regime to be realized [4]. It is obvious that knowledge of relaxation times and relaxation (non-steady-state) processes during EAS is essential for the successful development of practical applications of this highly unusual type of scattering.

Until recently, only estimates of relaxation times for EAS in uniform gratings have been made [2–4]. The analysis was based on physical assumptions and speculations [3, 4], rather than direct treatment of non-steady-state regime of EAS. Simple analytical equations for the relaxation times were derived [3, 4]. However, the accuracy of these equations is questionable, since their derivation did not take into account re-scattering processes in the grating. Moreover, these equations are not applicable in the presence of the additional resonances [5, 6, 8].

Therefore, the first aim of this paper is to present an efficient numerical algorithm for the rigorous analysis of non-steady-state EAS of bulk electromagnetic waves in wide uniform and non-uniform holographic gratings. The second aim is to investigate non-steady-state EAS and accurately determine relaxation times in narrow and wide uniform periodic gratings. In particular, amplitudes of the incident wave (0th diffracted order) and scattered wave (+1 diffracted order) inside and outside the grating will be determined as functions of time and coordinates after the incident wave is “switched on.”

2 Structure and methods of analysis

Consider an isotropic medium with a slab-like, uniform, holographic grating with a sinusoidal modulation of the dielectric permittivity (see fig 1):

$$\begin{aligned} \epsilon_s &= \epsilon + \epsilon_g \exp(iq_x x + iq_y y) + \epsilon_g^* \exp(-iq_x x - iq_y y), & \text{if } 0 < x < L, \\ \epsilon_s &= \epsilon, & \text{if } x < 0 \text{ or } x > L, \end{aligned} \quad (1)$$

where L is the grating width, ϵ_g is the grating amplitude, the mean dielectric permittivity ϵ is the same inside and outside the grating, q_x and q_y are the x and y components of the reciprocal lattice vector \mathbf{q} , $q = 2\pi/\Lambda$, Λ is the period of the grating, and the coordinate system is shown in figure 1. There is no dissipation in the medium (ϵ is real and positive), and the structure is infinite along the y and z axes.

Non-steady-state EAS in this structure occurs when the incident wave is switched on at some moment of time. Then, both the incident and scattered wave amplitudes inside and outside the grating evolve in time and gradually relax to their steady-state values at $t = +\infty$. This occurs when the incident pulse, having an infinite aperture along the y and z axes, is the product of a sinusoid and a step function of time.

However, the numerical analysis of this infinitely long (in time) pulse is inconvenient, since its Fourier transform contains a δ -function. Therefore, in order to calculate non-steady-state amplitudes of the incident and scattered waves in the structure at an arbitrary moment of time $t = t_0$, we consider a rectangular (in time) sinusoidal

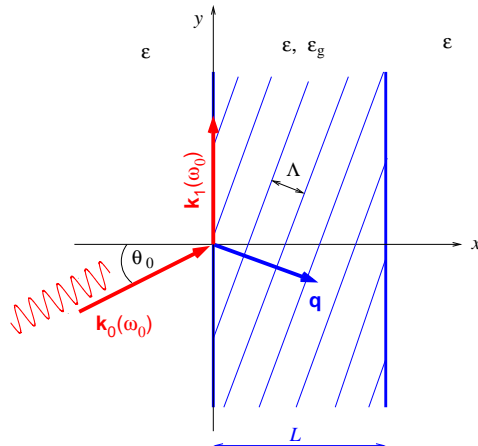


Fig. 1. The geometry of EAS in a slanted periodic grating.

incident pulse of time length $2t_0$, amplitude E_{00} , and angle of incidence θ_0 (fig. 1), which has a simple analytical Fourier transform. We also assume that the incident pulse is switched on instantaneously (with the amplitude E_{00}) everywhere in the grating. That is, we ignore the process of propagation of the pulse through the grating. This assumption allows a substantial reduction in computational time. It is correct only if the time t_0 , at which non-steady-state amplitudes are calculated, is significantly larger than $t_g = (L/\cos\theta_0)/(c\epsilon^{-1/2})$ – the time of propagation of the incident pulse across the grating. We will see below that this condition is satisfied (for most times) since typical relaxation times $\tau \gg t_g$.

Thus, at $t = 0$, the front of the pulse is at the rear grating boundary, i.e. the incident field is zero behind the grating (at $x > L$). This means that if the angle of incidence $\theta_0 \neq 0$ (fig. 1), then the amplitude of the incident pulse is not constant along a wave front. Therefore, the incident pulse experiences diffractive divergence, and the spatial Fourier transform should be used. However, this divergence can be ignored in our further considerations, since it may be significant only within several wavelengths near the front of the pulse, i.e. for times $\approx 10^{-14}$ s or smaller (this is the time for the pulse to travel a distance of a few wavelengths). This time is several orders of magnitude less than typical relaxation times (see below). Therefore, only for very short time intervals after switching an incident pulse on can noticeable errors result from the above approximations.

The frequency spectrum of this input is determined from its analytical Fourier transform. As a result, the incident pulse is represented by a superposition of an infinite number of plane waves having different frequencies and amplitudes, all incident at θ_0 . Note that the spectrum of the incident pulse depends on the pulse width $2t_0$, and is different for every time t_0 at which we calculate the fields. The steady-state response of the grating to each plane wave is determined by means of the rigorous theory of steady-state EAS [7], based on the enhanced T-matrix algorithm [10, 11], or the approximate theory [8] (if applicable). Thus the frequency spectrum of the incident and scattered waves inside and outside the grating is obtained, and their amplitudes as functions of the x -coordinate at any moment time can be found using the inverse Fourier transform. Due to the geometry of the problem, the non-steady-state incident and scattered wave amplitudes do not depend on the y -coordinate.

Note that the inverse Fourier transform is taken at $t = t_0$, i.e. at the middle of the incident pulse, in order to minimize numerical errors. The inverse Fourier transform is found by direct integration, to allow a non-uniform set of frequency points to be used. The rapid variation of the frequency spectra at certain points, and the wide frequency

spectrum of the input for small t_0 make it infeasible to use the fast Fourier transform. The calculations are carried out separately for each moment of time. Therefore, there is no accumulation of numerical errors, and the errors that are noticeable at small times $\approx 10^{-14}$ s (see above) disappear at larger times.

This approach is directly applicable for all shapes of the incident pulse, as well as for an incident beam of finite aperture. However, for beams of finite aperture, we should also use the spatial Fourier integral.

Since the approximate theory is directly applicable for all types of waves (including surface and guided waves in periodic groove arrays [2, 3, 9]), the developed approach to non-steady-state scattering is also applicable for all types of waves (if used together with the approximate theory).

3 Numerical Results

Using the described numerical algorithm, non-steady-state EAS of bulk TE electromagnetic waves in uniform holographic gratings given by eqn (1) has been analyzed. The grating parameters are as follows: $\epsilon = 5$, $\epsilon_g = 5 \times 10^{-3}$, $\theta_0 = 45^\circ$, and the wavelength in vacuum (corresponding to the central frequency ω_0 of the spectrum of the incident pulse) $\lambda_0 = 1 \mu\text{m}$. The Bragg condition is assumed to be satisfied precisely for the first diffracted order at $\omega = \omega_0$:

$$\mathbf{k}_1(\omega_0) = \mathbf{k}_0(\omega_0) - \mathbf{q}, \quad (2)$$

where $\mathbf{k}_0(\omega)$ are the frequency dependent wave vectors of the plane waves in the Fourier integral of the incident pulse, $\mathbf{k}_1(\omega)$ are the wave vectors of the corresponding first diffracted orders (scattered waves), $k_1(\omega_0) = k_0(\omega_0) = \omega_0 \epsilon^{1/2} / c$, $\mathbf{k}_1(\omega_0)$ is parallel to the grating boundaries (fig. 1), and c is the speed of light. Note that if $\omega \neq \omega_0$, $\mathbf{k}_1(\omega)$ is not parallel to the grating boundaries [8].

Typical relaxation of amplitudes of the scattered wave (+1 diffracted order) and incident wave (0th diffracted order) over time inside and outside the gratings of widths $L = 10 \mu\text{m}$, $28 \mu\text{m}$, and $80 \mu\text{m}$ is shown in the animations in fig. 2. The time dependencies of non-steady-state amplitudes of the scattered wave (+1 diffracted order) at $x = 0$, $L/2$, and L , and the transmitted wave (0th diffracted order at $x = L$) are shown in fig. 3 for the same grating widths. Note that $L = 28 \mu\text{m}$ is approximately equal to the critical width L_c [5]. Physically, $L_c/2$ is the distance within which the scattered wave can be spread across the grating by means of the diffractive divergence, before being re-scattered by the grating [5]. All the curves in figures 2 and 3 can equally be regarded as approximate or rigorous, since both the theories in the considered structure give practically indistinguishable results [7].

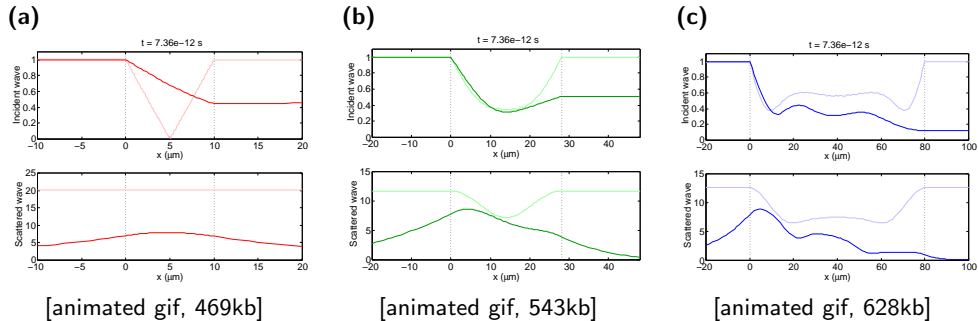


Fig. 2. Animations showing the approach of amplitudes of the scattered (bottom graphs) and incident (top graphs) waves to the steady-state solutions (light lines). The grating widths are (a) $L = 10 \mu\text{m}$, (b) $L = 28 \mu\text{m} \approx L_c$, and (c) $L = 80 \mu\text{m}$. The vertical dotted lines show the grating boundaries.

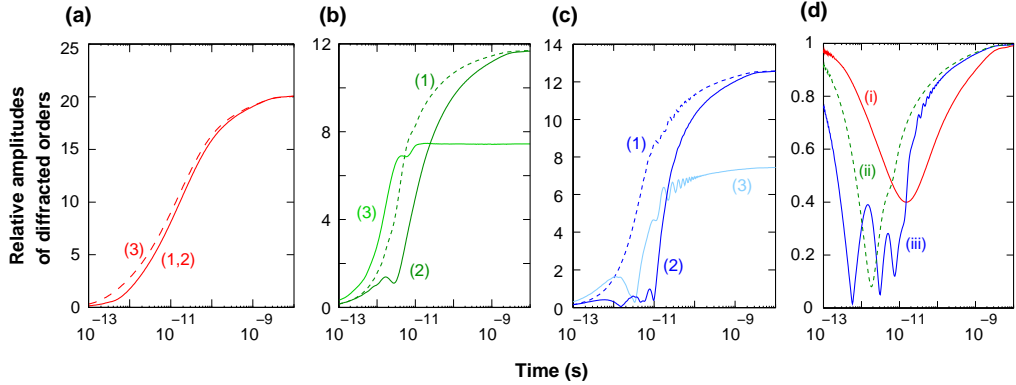


Fig. 3. The time dependencies of normalized non-steady-state amplitudes of **(a–c)** the first diffracted order (scattered wave) $|E_1/E_{00}|$, and **(d)** the zeroth diffracted order (transmitted wave) $|E_0(x=L)/E_{00}|$. The grating widths are $L = 10 \mu\text{m}$ (**(a)** and curve (i) in **(d)**), $L = 28 \mu\text{m} \approx L_c$ (**(b)** and curve (ii) in **(d)**), and $L = 80 \mu\text{m}$ (**(c)** and curve (iii) in **(d)**). The scattered wave amplitudes **(a–c)** are shown at (1) the front boundary ($x = 0$), (2) the rear boundary ($x = L$), and (3) the middle of the grating ($x = L/2$).

If $L < L_c$, then the relaxation at the front and rear grating boundaries occurs practically simultaneously (see figures 2(a) and 3(a)). In the middle of the grating, the scattered wave amplitude grows slightly faster at small t . This is due to energy losses from the scattered wave, caused by diffractive divergence of the wave near the boundaries (the edges of the scattered beam). This effect becomes more obvious with increasing grating width, and is especially strong if $L \approx L_c$ (fig. 3(b)). This is because the effect of the diffractive divergence in the middle of the grating (in the middle of the beam) becomes weaker with increasing grating width (i.e. beam aperture). At the same time, at the edges of the beam (at the grating boundaries) the divergence is strong, resulting in a significant reduction of the rate of change of the non-steady-state scattered wave amplitudes (compare curves (1) and (2) with curve (3) in fig. 3(b)). However, in wide gratings (with $L > L_c$), the relaxation occurs first near the front boundary, and then the steady-state scattered wave amplitudes start spreading towards the rear boundary (fig. 2(c)). Therefore, the relaxation process in the middle of the grating and especially at the rear boundary tends to slow down compared to that near the front boundary – compare curves (1) and (2) in figs. 3(b,c).

The relaxation near the front boundary takes place more or less smoothly, except for some not very significant oscillations in wide gratings near the end of the relaxation process (curves (1) in figs. 3(a–c)). The same happens in the middle of the grating and at the rear boundary in narrow gratings ($L < L_c$). However, if $L \geq L_c$, the relaxation curves in the middle of the grating and at the rear boundary display a complex and unusual behavior at small and large time intervals (see curves (2) and (3) in figs. 3(b,c)).

The unusual and complex character of relaxation processes in wide gratings is especially obvious from the time dependencies of non-steady-state incident (transmitted) wave amplitude at the rear grating boundary (figs. 2(c), 3(d)). In wide gratings, these dependencies are characterized by significant oscillations with minima that are close to zero – see fig. 2(c) and curve (iii) in fig. 3(d). The typical number of these oscillations increases with increasing grating width (compare curves (ii) and (iii) in fig. 3(d)). The minima in these oscillations tend to zero with increasing L . When the amplitude of the transmitted wave at the rear grating boundary is close to zero, almost all energy of the incident wave is transferred to the scattered wave. In wide gratings this may happen several times during the relaxation process (figs. 2(c), 3(d)).

The relaxation times at the grating boundaries and at $x = L/2$, determined as the

times at which the amplitudes reach $(1 - 1/e)$ of their steady-state values, are:

L	$\tau _{x=0}$	$\tau _{x=L/2}$	$\tau _{x=L}$
$10 \mu\text{m}$	$4 \times 10^{-11} \text{ s}$	$4 \times 10^{-11} \text{ s}$	$4 \times 10^{-11} \text{ s}$
$28 \mu\text{m}$	$6 \times 10^{-12} \text{ s}$	$1.7 \times 10^{-12} \text{ s}$	$2.4 \times 10^{-11} \text{ s}$
$80 \mu\text{m}$	$7.4 \times 10^{-12} \text{ s}$	$1.2 \times 10^{-11} \text{ s}$	$3.4 \times 10^{-11} \text{ s}$

The relaxation times for narrow gratings, determined by means of the developed algorithm, are about three times smaller than those previously estimated [4]. The significant overestimation of relaxation times in paper [4] is due to not taking into account the effects of re-scattering of the scattered wave in the grating. Re-scattering reduces the transmitted wave amplitude during the relaxation process (fig. 3(d)). Thus, the energy flow into the scattered wave is increased, and the relaxation times are reduced (for more detailed discussion of re-scattering see [5]).

During the process of relaxation, the scattered wave propagates a particular distance along the y -axis. Therefore, the relaxation times determine critical apertures l_c (along the y -axis) of the incident beam, that are required for steady-state EAS to be achieved (see also [4]). For example, for fig. 3(a) (with the largest values of τ), the critical aperture of the incident beam is $l_c = c\tau\epsilon^{-1/2} \cos \theta_0 \approx 0.4 \text{ cm}$, which does not present any problem in practice.

4 Conclusions

This paper has developed an efficient numerical algorithm for the approximate and rigorous numerical analysis of non-steady-state EAS of waves in uniform slanted gratings. An unusual type of relaxation with strong oscillations of the incident and scattered wave amplitudes has been predicted for gratings wider than the critical width.

If used in conjunction with the approximate theory of steady-state EAS [2–4, 8], the developed algorithm is immediately applicable for the analysis of non-steady-state EAS of all types of waves, including surface and guided modes in periodic groove arrays.

Typical relaxation times have been calculated for narrow and wide gratings. It has been shown that these times are significantly smaller than previous estimates [3, 4]. The corresponding critical apertures of the incident beam that are required for achieving steady-state EAS have also been determined. The obtained results demonstrate that steady-state EAS can readily be achieved in practice for reasonable beam apertures and not very long gratings.

References and links

1. S. Kishino, A. Noda, and K. Kohra, "Anomalous enhancement of transmitted intensity of diffraction of x-rays from a single crystal," *J. Phys. Soc. Japan.* **33** 158–166 (1972).
2. M. P. Bakhturin, L. A. Chernozatonskii, and D. K. Gramotnev, "Planar optical waveguides coupled by means of Bragg scattering," *Appl. Opt.* **34** 2692–2703 (1995).
3. D. K. Gramotnev, "Extremely asymmetrical scattering of Rayleigh waves in periodic groove arrays," *Phys. Lett. A*, **200** 184–190 (1995).
4. D. K. Gramotnev, "A new method of analysis of extremely asymmetrical scattering of waves in periodic Bragg arrays," *J. Physics D* **30** 2056–2062 (1997).
5. D. K. Gramotnev and D. F. P. Pile, "Double-resonant extremely asymmetrical scattering of electromagnetic waves in non-uniform periodic arrays," *Opt. Quant. Electron.* **32** 1097–1124 (2000).
6. D. K. Gramotnev, "Grazing-angle scattering of electromagnetic waves in periodic Bragg arrays," *Opt. Quant. Electron.* **33** 253–288 (2001).
7. T. A. Nieminen and D. K. Gramotnev, "Rigorous analysis of extremely asymmetrical scattering of electromagnetic waves in slanted periodic gratings," *Opt. Commun.* **189** 175–186 (2001).
8. D. K. Gramotnev, "Frequency response of extremely asymmetrical scattering of electromagnetic waves in periodic gratings," in *Diffraction Optics and Micro-Optics*, OSA Technical Digest (Optical Society of America, Washington DC, 2000), pp. 165–167.
9. D. K. Gramotnev, T. A. Nieminen, and T. A. Hopper, "Extremely asymmetrical scattering in gratings with varying mean structural parameters," *J. Mod. Opt.* **49** 1567–1585 (2002).

10. M. G. Moharam, E. B. Grann, D. A. Pommet, and T. K. Gaylord, "Formulation for stable and efficient implementation of the rigorous coupled-wave analysis of binary gratings," *J. Opt. Soc. Am. A* **12** 1068–1076 (1995).
 11. M. G. Moharam, D. A. Pommet, E. B. Grann, and T. K. Gaylord, "Stable implementation of the rigorous coupled-wave analysis for surface-relief dielectric gratings: enhanced transmittance matrix approach," *J. Opt. Soc. Am. A* **12** 1077–1086 (1995).
-